



AAPM/RSNA Physics Tutorial for Residents: Topics in CT

Image Processing in CT¹

Dianna D. Cody, PhD

Several image-processing methods for computed tomographic (CT) examinations are currently being used in clinical radiology departments. Image processing involves operations such as reformatting of original CT images, volume-rendered displays, surface-rendered displays, and physiologic imaging analysis. The reformatting process does not alter the CT voxels in any way; instead it uses them in off-axis views and displays the images produced from the original reconstruction process in an orientation other than how they were originally generated. Sagittal, coronal, oblique, and curved reformatting are standard reformatting methods. Other reformatting techniques include maximum-intensity projection, minimum-intensity projection, and variable thickness viewing. Volume and surface rendering are two different methods for reformatting axial images into three-dimensional views. CT perfusion allows the measurement of physiologic parameters over time. Additional postprocessing efforts can potentially add value to the patients and their outcomes, as can be seen in the cases that illustrate this article.

©RSNA, 2002

Index terms: Computed tomography (CT), image processing • Image processing

RadioGraphics 2002; 22:1255–1268

¹From the Division of Diagnostic Imaging, Department of Imaging Physics, University of Texas M. D. Anderson Cancer Center, 1515 Holcombe Blvd, Box 56, Houston, TX 77030-4009. From the AAPM/RSNA Physics Tutorial at the 2001 RSNA scientific assembly. Received March 21, 2002; revision requested April 29 and received May 21; accepted May 24. **Address correspondence** to the author (e-mail: dcody@mdanderson.org).

©RSNA, 2002

Introduction

Image-processing methods have become relatively easy to use. Computed tomographic (CT) images are often well suited to postprocessing. Most postprocessing for CT is accomplished by using image-reformatting techniques. There are several CT image-reformatting approaches (eg, sagittal/coronal, oblique, curved, and variable thickness viewing) that help to orient radiologists and referring physicians to particular anatomic structures. Other image-processing methods that are useful clinically for CT images include volume rendering, surface rendering, and physiologic imaging (CT perfusion). Each of these methods is briefly described here, and actual clinical examples of each are presented. Cases were selected specifically for instances in which the postprocessing effort resulted in some added value to the patient or enhanced the CT examination in a specific manner.

The CT scanner acquisition parameters that have the most direct effect on the quality of the image-processing result are section thickness and section interval. Pitch has less of an effect, but higher pitches can introduce artifacts, such as zebra-type striping, which is the most apparent artifact. (Pitch is defined as the collimation thickness in the z direction exposed during a single revolution of the x-ray tube divided by the table travel distance.) The ability of multiple-row detector CT scanners to cover large areas rapidly has resulted in the generation of large numbers of thin sections with small image intervals (several hundred to a thousand) that produce exquisite postprocessing results; however, the increased overhead involved in transferring and archiving immense data sets from these examinations must be recognized.

Reformatting Approaches

The usefulness of the reformatting process is underappreciated by the radiologic community. The

ability to view a CT image sequence from a perspective other than the axial acquisition plane is useful for even an experienced radiologist on occasion (1–5). In general, the reformatting process does not alter the CT voxels in any way; instead it uses these voxels in off-axis views. The term *reconstruction* is often used, although it is inaccurate in this context. The reconstruction process, especially in CT, refers to a very specific procedure that converts raw projection data into an axial image. Reformatting, on the other hand, merely displays the images produced from the original reconstruction process in an orientation other than how they were originally produced.

Sagittal and Coronal Reformatting

The routine reformatting of a sequence, or stack, of CT images into standard orthogonal, sagittal, and coronal views is illustrated in Figure 1. In this view, the x direction of an axial image plane is along the patient's right-left axis, the y direction of an axial image plane is along the patient's anterior-posterior axis, and the z direction of the axial image plane is along the patient's superior-inferior axis.

A sagittal view is formed from a stack of CT images by sampling in the y and z directions (Fig 1). Similarly, a coronal view is constructed from a stack of CT images by sampling in the x and z directions. These views can look somewhat distorted if the voxel dimensions are not isotropic. Often, the section thickness is larger than the pixel dimension, which can produce a stair-step appearance in the reformatted view.

In Figure 2a (a subsection of an axial image from a CT pulmonary arteriography examination), one of the findings was identified as a potential embolus. The coronal reformatted image in Figure 2b illustrates clearly that the potential embolus was actually a linear scan artifact, which can also be seen as a horizontal low-attenuation line extending from the vertebral endplates. In this case, the patient clearly benefited from the postprocessing effort, since unnecessary treatment for a pulmonary embolus that did not exist was avoided.

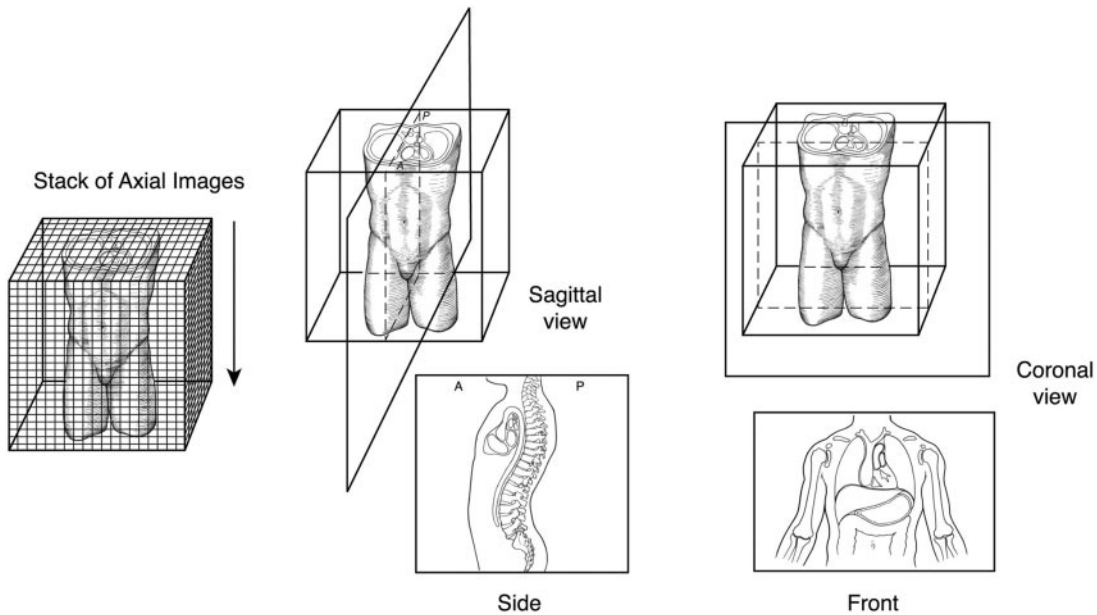
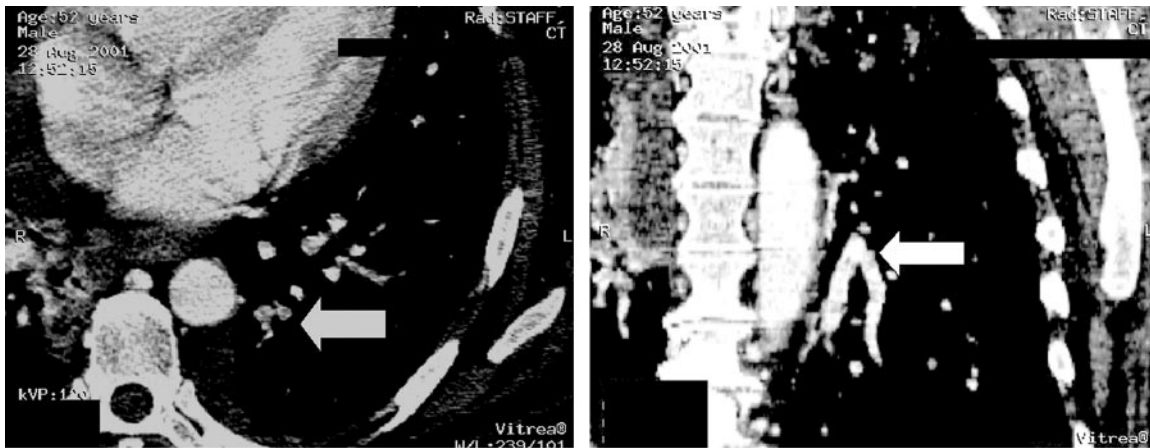


Figure 1. Diagram illustrates how a sequence of axial images can be considered to form a vertical “stack.” By sampling a three-dimensional stack of CT numbers along the y-z plane, sagittal views can be generated. Similarly, sampling in the x-z plane generates coronal views. The CT reformatting process is thus fundamentally different (and simpler) than the CT reconstruction process (in which raw CT projection signal data are used to create an axial image), and these two terms (*reformat* and *reconstruction*) should not be used interchangeably.



a. **Figure 2.** (a) Multiple-row detector CT pulmonary arteriogram demonstrates low attenuation within pulmonary arterioles (arrow), a finding suspicious for pulmonary embolus. Axial images were acquired with 1.25-mm section thickness at a pitch of 1.5. (b) Coronal reformatted view reveals that the suspected pulmonary embolus was actually part of a linear scan artifact (arrow) extending in the x direction. This artifact also appears at the level of the vertebral endplates. (Case courtesy of Gregory Gladish, MD, University of Texas M. D. Anderson Cancer Center, Houston.)

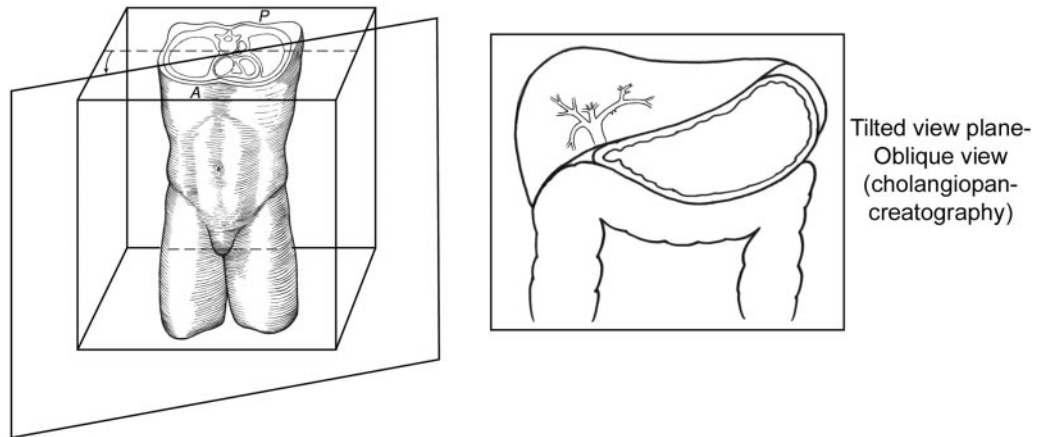
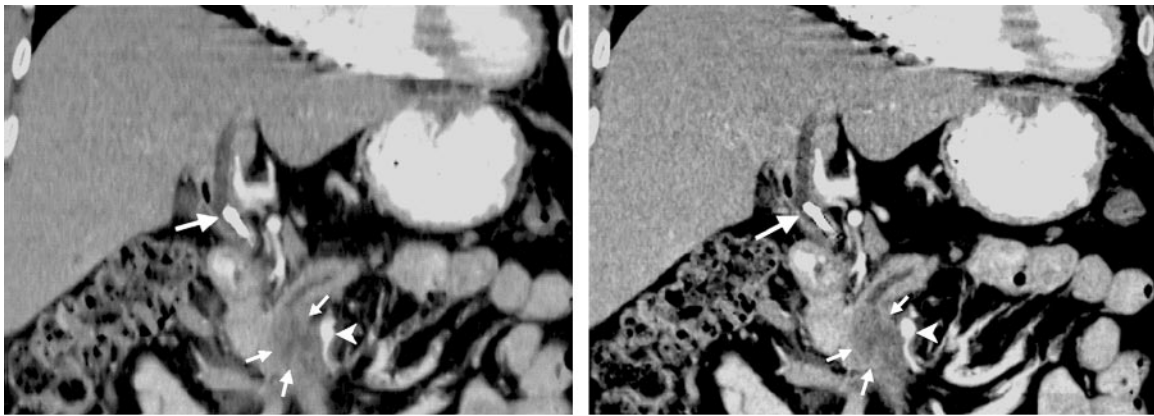


Figure 3. Diagram illustrates how a stack of axial CT images can also be sampled in more arbitrary ways, for example, on an angle between the x and y axes and along the z axis. The pancreatic anatomy is particularly well visualized along this tilted plane.



a. **Figure 4.** (a) Oblique reformatted view was obtained by using axial images (reconstructed from a helical acquisition) obtained at 2.5-mm section thickness and a pitch of 1.5. A portion of a stent (large arrow) and a tumor (small arrows) are seen adjacent to the superior mesenteric artery (arrowhead). (b) On another oblique reformatted view obtained by using the same axial source images but reconstructed to 1.25 mm thickness, the stent (large arrow) and the tumor (small arrows) are much better visualized, as is the involvement of the superior mesenteric artery (arrowhead). The data set for this image required no additional scan time and yielded reformatted images of a perceptibly sharper quality. (Case courtesy of Eric Tamm, MD, University of Texas M. D. Anderson Cancer Center, Houston.)

Oblique Reformating

Oblique reformating is quite similar to sagittal or coronal reformating, except that the CT voxels in the stack are sampled along an axis that is tilted from either the x or y plane (Fig 3). Several organ systems in the human body are not especially well visualized with routine sagittal and coronal planes, and oblique reformating can be useful in these instances.

For example, the hepatic and pancreatic regions are well visualized with oblique reformatted views. The oblique view in Figure 4a shows the liver, the placement of a portion of a stent, the location of a tumor, and the location of the superior mesenteric artery. The CT image sequence was obtained by using a 2.5-mm section thickness and a pitch of 1.5. Noticeable improvement can be appreciated in Figure 4b, which represents the same patient as in Figure 4a, but with a different CT image sequence (section thickness of 1.25

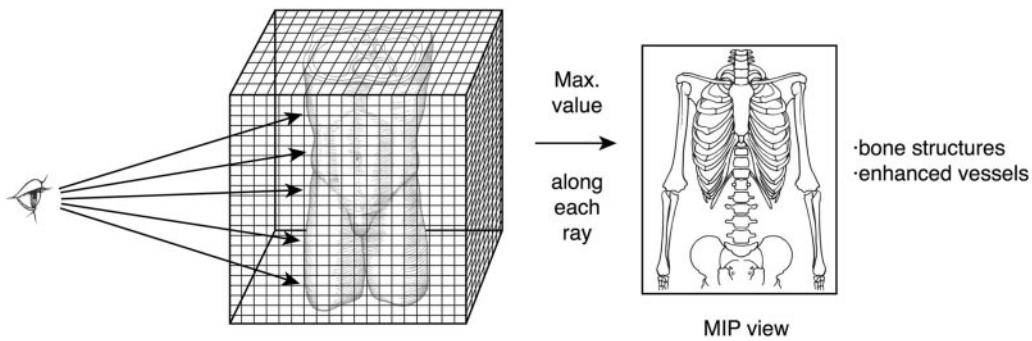
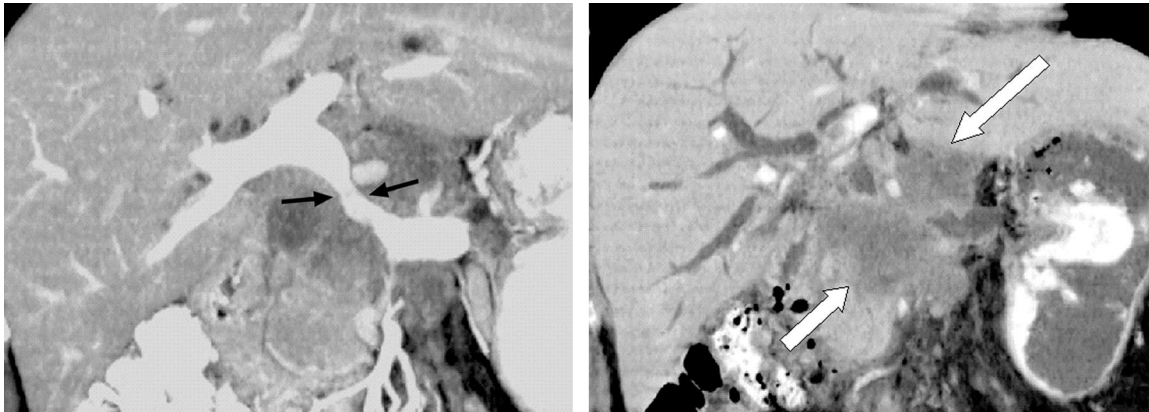


Figure 5. Diagram illustrates maximum-intensity projection, one of the methods for viewing re-formatted and three-dimensional images. This method tends to accentuate highly attenuating structures such as bone and contrast material–enhanced vasculature.



a. **Figure 6.** (a) Oblique maximum-intensity projection of a slab (cropped volume) of the hepatic and pancreatic regions clearly demonstrates the enhancing regional vasculature and orally administered gastrointestinal contrast material. The image clearly shows vascular stenosis (arrows) caused by a surrounding tumor, but the tumor margins are not well seen. (b) Oblique minimum-intensity projection (slab view) of the same patient emphasizes the hepatic biliary tree. The tumor margins (arrows) are delineated better with this technique. A slightly different slab view volume was used in this view. (Case courtesy of Eric Tamm, MD, University of Texas M. D. Anderson Cancer Center, Houston.)

mm and a pitch of 1.5). Figure 4b is sharper than Figure 4a and provides a higher-quality image of the involvement of the superior mesenteric artery and tumor region.

Maximum- and Minimum-Intensity Projections

Reformatted images and several other three-dimensional images can be displayed with several different methods on current commercial image-processing workstations. The two viewing methods most often used are the maximum-intensity projection and the minimum-intensity projection. In the maximum-intensity projection method, viewing rays are traced from the expected position

of the operator through the object to the display screen, and only the relative maximum value detected along each ray path is retained by the computer (Fig 5). This method tends to display bone and contrast material–filled structures preferentially, and other lower-attenuation structures are not well visualized. Similarly, minimum-intensity projection involves detecting the minimum value along the ray paths in each view. Both methods can add different and important information to the original axial sequence.

For example, the maximum-intensity projection image in Figure 6a shows the vasculature of

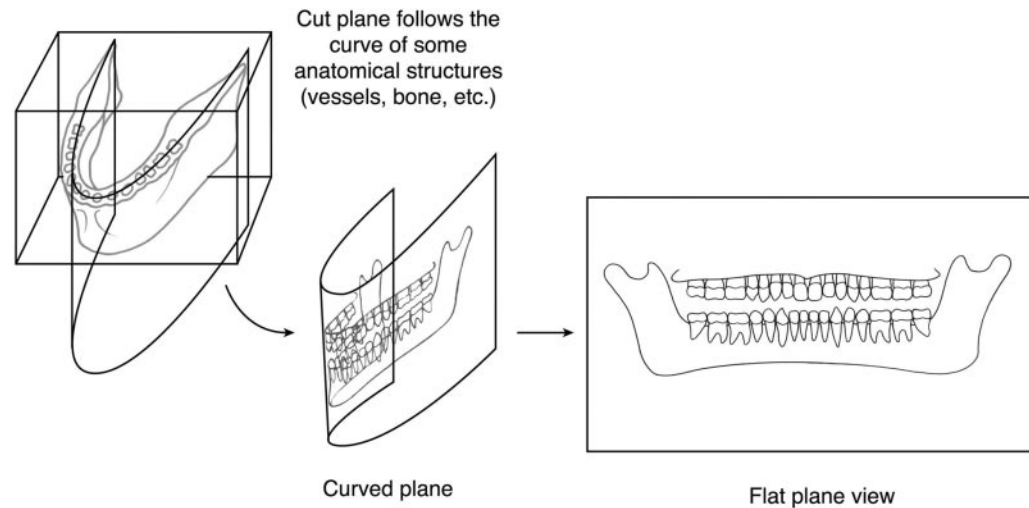


Figure 7. Diagram illustrates how a stack of axial CT images can be sampled along a curved plane. The case illustrated is a simulated panoramic view of the mandible.

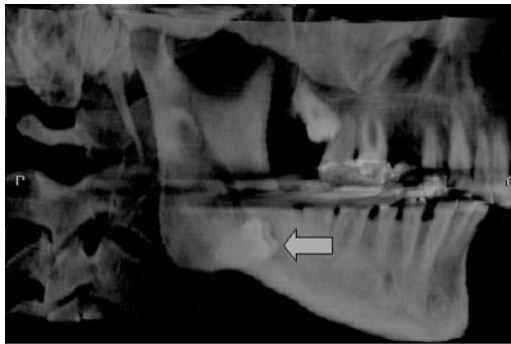
the hepatic and pancreatic regions quite clearly. Likewise, the narrowing of a major vessel caused by a surrounding lesion is easily observed, but the margins of the lesion are not. On a minimum-intensity projection (Fig 6b) of the same oblique view, the vasculature is no longer visible, but the hepatic biliary tree has appeared and the margins of the lesion are also much more apparent. These oblique views, both the maximum-intensity projection and the minimum-intensity projection, offer radiologists, referring physicians, and surgeons an alternate view of the patient's anatomy and pathologic condition, which can save time in the operating room, benefiting the patient directly.

Curved Reformatting

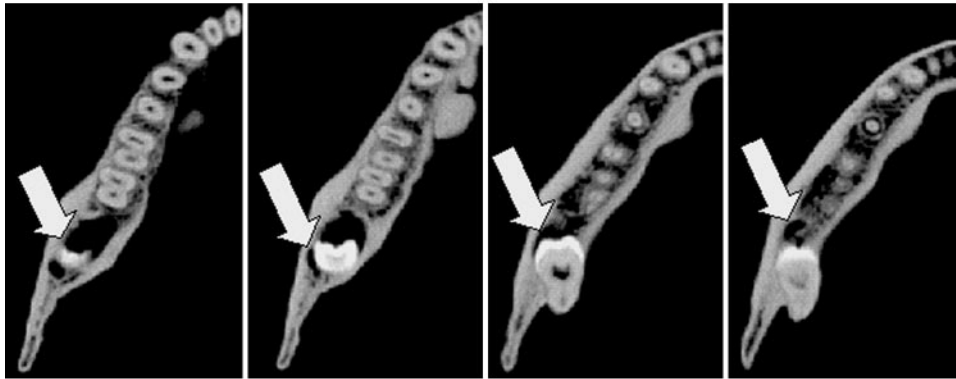
It is also possible to sample a three-dimensional stack of CT images along a curved plane. The technique can be especially useful when narrowing of tortuous tubular structures (eg, blood vessels) is suspected. The desired curve is generally defined along some anatomic structure, such as

the curve of the mandible (Fig 7). Other typical curves used for this application include the midline of a vessel in three-dimensional space, along an implanted stent, and along the spinal cord.

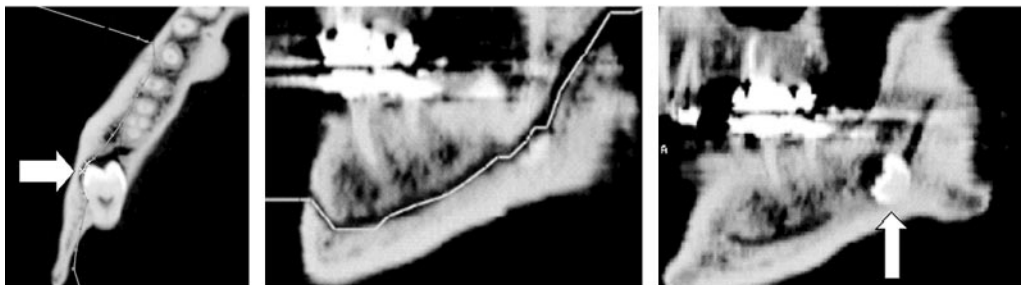
The case in Figure 8 represents special three-dimensional image processing of the jaw of a patient about to undergo oral surgery for an impacted molar. The oral surgeon was planning to approach the procedure from the lateral side, which is easier to access surgically. On the panoramic dental radiograph, it was not clear which way the alveolar nerve passed by the tooth. On the axial CT images (Fig 8b, 8c), the alveolar nerve was followed three dimensionally; on the curved reformatted image (Fig 8d), it became clear that the nerve passed lateral to the tooth. Performing the surgery from the original lateral approach would have placed the nerve right in the path to the tooth, so it was performed from the lingual approach instead. Although this approach is technically more difficult, with the advanced knowledge of the location of the nerve, the surgeon was able to quickly cut to the tooth without stopping and inspecting frequently for the nerve. This knowledge saved about 45 minutes of operating room time and furthermore preserved the nerve.



a.



b.



c.

d.

e.

Figure 8. (a) Lateral transparent volume-rendered image reformatted from the axial CT images demonstrates an impacted molar (arrow). (b, c) Axial images were used to locate the alveolar nerve canal (arrows) and define the formatting curve (gray line in c). (d) Curved reformatted image demonstrates the alveolar nerve canal in its entirety (gray line). (e) Image of the plane just lingual to the alveolar nerve canal reveals the impacted molar (arrow). (Case courtesy of Gordon Harris, PhD, Harvard Medical School and Massachusetts General Hospital, Boston.)

Variable Thickness Viewing

The speed of multiple-row detector CT scanners has prompted the idea that if CT images are acquired at their smallest possible section thickness, they can be viewed as “slabs” by combining mul-

tiple images to improve noise and co-planar effects (Fig 9). The milliampere seconds (mAs) can also be reduced proportionately for the acquisition of thin sections, so that radiation exposure

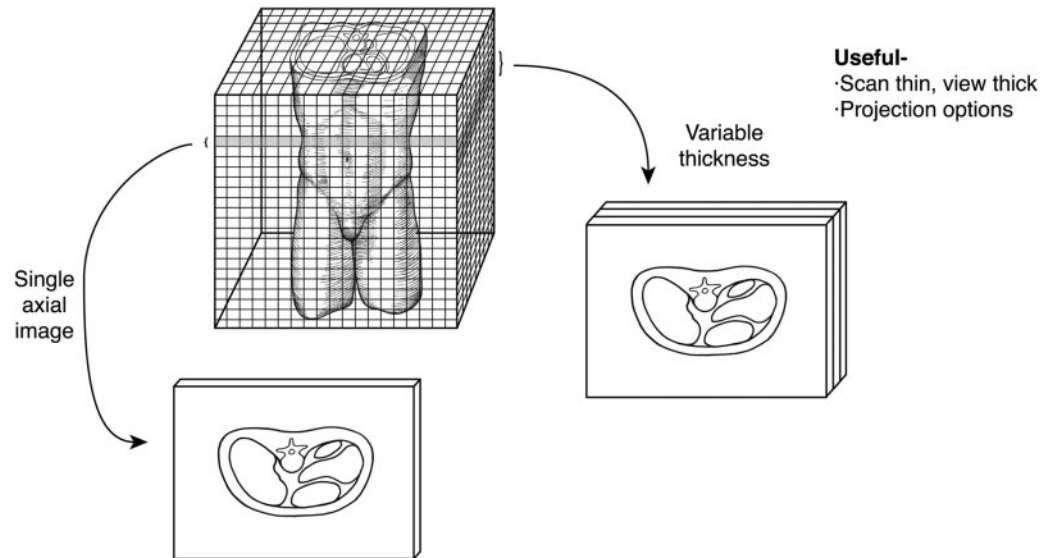


Figure 9. Diagram illustrates the concept of variable thickness viewing; that is, scans are obtained with decreased section thickness (and lower milliampere seconds) and then viewed in multiples (two or more combined). This method results in images of superior quality compared with images of equivalent thickness. The number of images that are averaged is generally variable, and this combination can be smoothly scrolled through the entire sequence of thin images. Although the number of images averaged can be variable, any combination allows smoother and quicker visualization of the entire sequence of thin images than does individual image review.

would not be significantly increased by the use of a less dose-efficient detector configuration. This technique would be useful for examinations such as lung cancer screening CT, because thin sections improve lesion detection and the accuracy of lesion volume measurement, as well as the image quality of variable thickness viewing. Another advantage of this approach is that if the images are routinely interpreted in the “slab” mode and something suspicious is detected, the thinner original images can easily be examined for a more detailed view instead of calling the patient back for an additional examination.

In the lung cancer screening case in Figure 10, a small part of the entire image has been enlarged to improve the visibility of fine structures. Several isolated nodular areas observed in the thin images (Fig 10a) were clearly vascular structures when viewed in the thicker plane (Fig 10b). A fissure (a rather indistinct linear structure) that was barely apparent on the thicker view was more easily visualized on the thinner image.

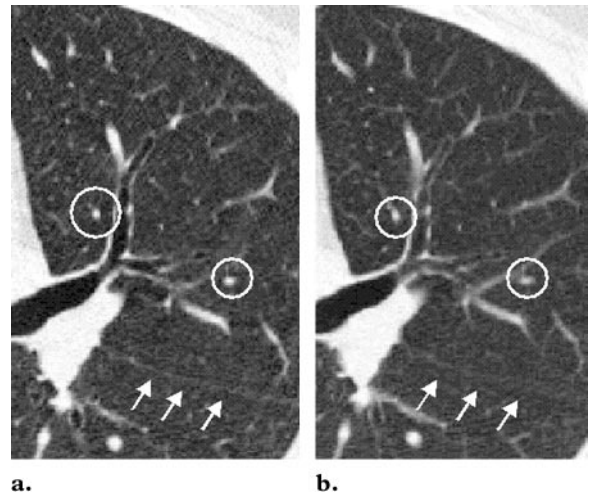


Figure 10. (a) Multiple-row detector CT scan acquired at 1.25-mm section thickness and a pitch of 1.5 reveals two possible nodules (within the circles). Note the sharply defined pleural fissure (arrows). (b) Image produced with variable thickness viewing (ie, averaging three images together to create a thicker image) demonstrates decreased image noise and shows that the possible nodules are vascular structures (within the circles). However, the fissure (arrows) is not visualized as well. (Case courtesy of Reginald Munden, MD, University of Texas M. D. Anderson Cancer Center, Houston.)

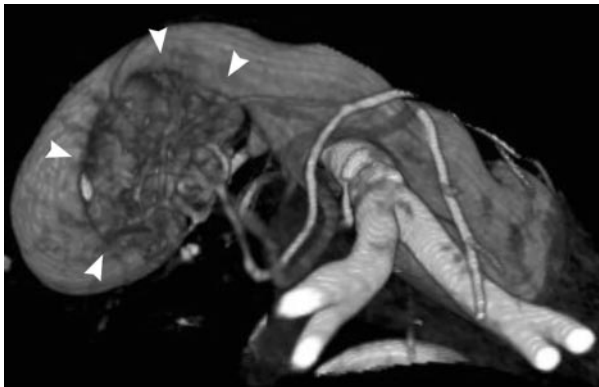
Figure 11. (a) Frontal volume-rendered image of a patient with horseshoe kidney who was scheduled to undergo surgery for a mass in the right posterior-inferior aspect of the fused kidney (arrowheads). The aorta is readily apparent (arrow). (b) Another view is somewhat closer and more superior than the view seen in a, and the kidney tissue has been rendered slightly more transparent. The unusual vasculature pattern in this case is readily apparent, with two upper pole arteries (open arrows) and two lower pole arteries (arrowheads) originating below the inferior mesenteric artery (solid arrow). (c) Volume-rendered view is from the inferior aspect of the patient and looking toward the superior direction. The vessels supplying the tumor region (arrowheads) can be clearly appreciated from this aspect. (Case courtesy of Marc Fenstermacher, MD, University of Texas M. D. Anderson Cancer Center, Houston.)



a.



b.



c.

Volume Rendering

Volume rendering has replaced most earlier applications of surface rendering with a few notable exceptions (ie, virtual colonoscopy and bronchoscopy and interior vessel analysis). Surface rendering remains useful for these few very specific three-dimensional applications. In volume rendering, the CT numbers that make up the image are assigned to be either visible or invisible, to be displayed with varying colors, and often to be displayed with varying opacity levels (transparency). The assignment of these characteristics to the

voxels can be defined for specific imaging protocols and organ systems (6–13). Vendors have developed independent workstations and software that can display these three-dimensional images quickly, and they generally have some flexibility in terms of the thresholding parameters (ie, which voxels become visible). Color maps and transparency levels can be more difficult to control for individual cases. Another useful option for volume rendering is the positioning of a spherical clipping volume, which sets a boundary between the voxels to remain visible (tissues inside the sphere) and voxels to be rendered invisible (all surrounding tissues). Three-dimensional image display for vascular anatomy provides excellent anatomic information for surgical planning. The patients in all three of the following examples benefited by having their surgical teams clearly understand and anticipate their anatomy, which resulted in well-planned operations.

In a case of horseshoe kidney, volume rendering with a monochrome three-dimensional display and with adjustment of opacity levels was very useful (Fig 11). The aorta and very unusual

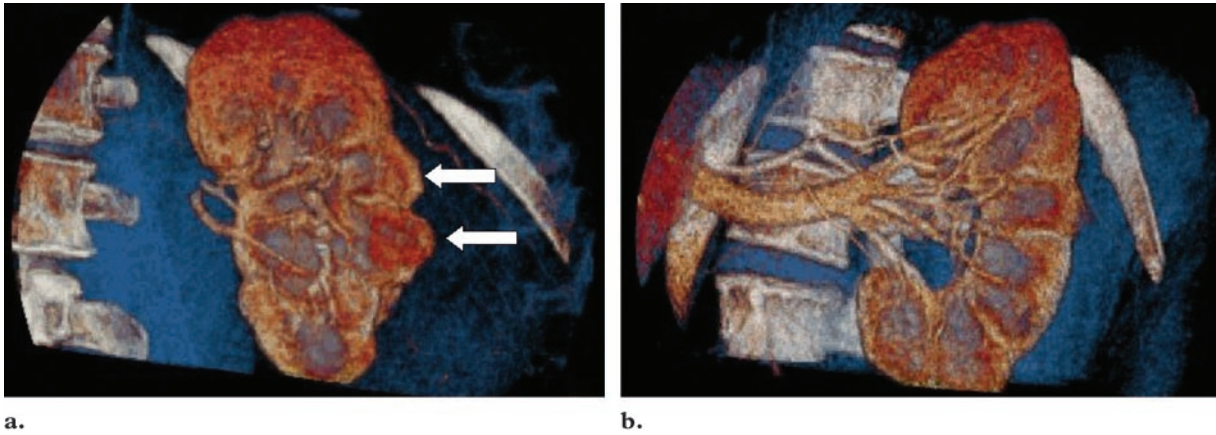


Figure 12. (a) Volume-rendered image for which the color map function was adjusted to help enhance the visibility of the tumors (arrows) on the cortex of the kidney. The kidney is shown as orange, the renal lesions are reddish, and the bones are white. Observing this case in motion (rotating right to left) helped the viewer appreciate the depth and interconnections of the anatomic structures. (b) An alternate frame of the movie loop from this case demonstrates the renal artery structure. (Case courtesy of Chuslip Charnsangavej, MD, University of Texas M. D. Anderson Cancer Center, Houston.)

vasculature patterns were well visualized (Fig 11a, 11b), which helped the surgeon prepare the approach and plan the operation. Another view from a posterior perspective toward the anterior direction offered the surgeon a realistic picture of the vasculature structure supplying the tumor region in the horseshoe kidney (Fig 11c). The workstation used to prepare this case (Vitrea; Vital Images, Plymouth, MN) also provides Web-based reports and has the capability to create compact disks that can be viewed in the operating room environment.

Surgeons often appreciate a three-dimensional representation of anatomy much more than radiologists, as it is much more similar to their visual experience in the operating room environment. In Figure 12, the color map function of volume rendering was adjusted to help the surgeon identify the location of several lesions relative to important surrounding structures. This type of image is more dramatic as an oscillating movie loop, as the motion seems to convey more depth information. The spherical clipping tool (also called a “shutter tool”) was applied in this example (Advantage Windows; GE Medical Systems, Milwaukee, Wis).

In Figure 13, a multiple-row detector CT series was processed to display a stenosis of the celiac axis (median arcuate ligament syndrome). Optimal contrast enhancement is critical in this type of imaging, which is more readily accomplished with multiple-row detector CT scanners because of their increased scanning speed. The shutter tool (Advantage Windows) was also applied in this example.

Surface Rendering

In surface rendering, the voxels located on the edge of a structure are identified, usually by intensity thresholding, and possibly enhanced with morphologic filtering or connectivity, and these voxels are displayed. The remaining voxels in the image are usually invisible. This approach is quite useful for examining tubular structures, such as the inside surfaces of airways (virtual bronchoscopy), the colon (virtual colonoscopy), and blood vessels (14,15). The thresholding assignment of the voxels that will be visible is both critical and sometimes difficult to reproducibly define. If the thresholding process is too aggressive, actual protruding structures can be lost from view because of partial volume effects. If the thresholding process is too lax, nontissue materials (eg, fluids) can

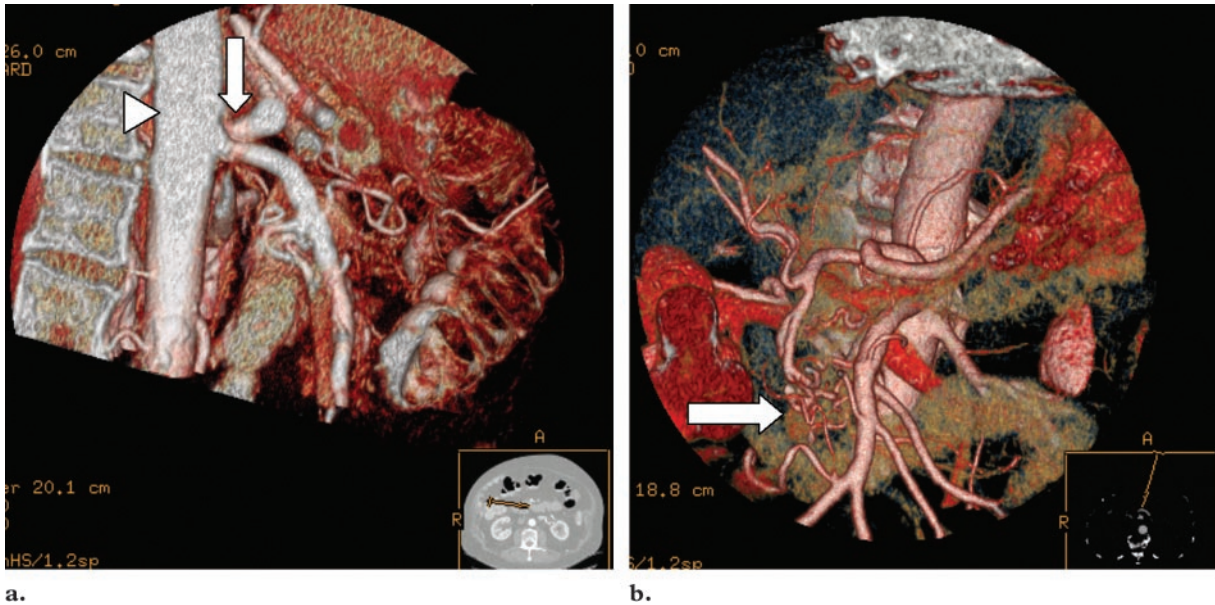


Figure 13. (a) Lateral volume-rendered view from a multiple-row detector CT series demonstrates severe stenosis of the celiac axis (arrow). This vessel was clipped orthogonally just beyond the stenotic area in the region of enlargement. The aorta (arrowhead) is also very apparent in this view. (b) Frontal volume-rendered view reveals collateral vessel development (arrow) to help supply the liver because of the severe stenosis in the celiac axis. (Case courtesy of Chuslip Charnsangavej, MD, University of Texas M. D. Anderson Cancer Center, Houston.)

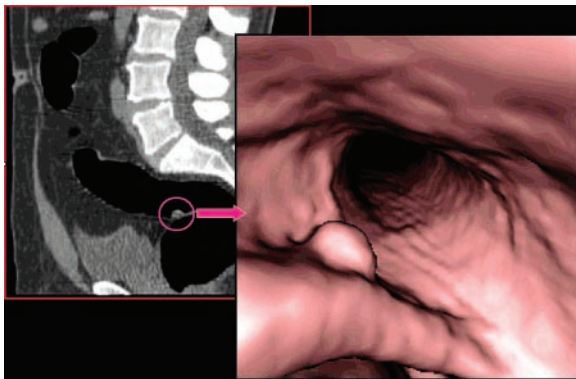


Figure 14. On the left, a two-dimensional sagittal reformatted view from a CT colonography examination shows a polypoid projection into the colonic lumen (red circle) that did not extend through the colonic wall. On the right, a three-dimensional endoluminal surface-rendered image from the “fly-through” sequence provides an enlarged view of the lesion, which later proved to be an adenomatous polyp at endoscopic biopsy. (Case courtesy of Revathy Iyer, MD, University of Texas M. D. Anderson Cancer Center, Houston.)

be rendered as if they were tissue, which can obscure protruding structures. New contrast materials have recently been introduced that can be

used by some automatic virtual colonoscopy programs to identify and remove remaining stool and fluids. Actual (true) tissue color cannot be automatically relayed in any of these situations. This aspect of CT will never match real endoscopic procedures.

Images from a virtual colonoscopy case are shown in Figure 14. Navigation through the colon can be somewhat awkward on some workstations, especially in cases in which the colon was not completely air-filled during the image acquisition period. If there are collapsed regions or filled areas, automated software often fails.

In a case of a cerebellar artery aneurysm, a surface-rendered view is used to illustrate the location of the aneurysm relative to a main branch structure (Fig 15a). The approach to this aneurysm was complicated by its location, but a view from the interior of the artery revealed the relative locations of the main artery, the neck of the aneurysm, and the branching artery (Fig 15b). This view was especially helpful for the interventional team in planning their approach to the aneurysm, and the patient benefited because the surgical team was well prepared.

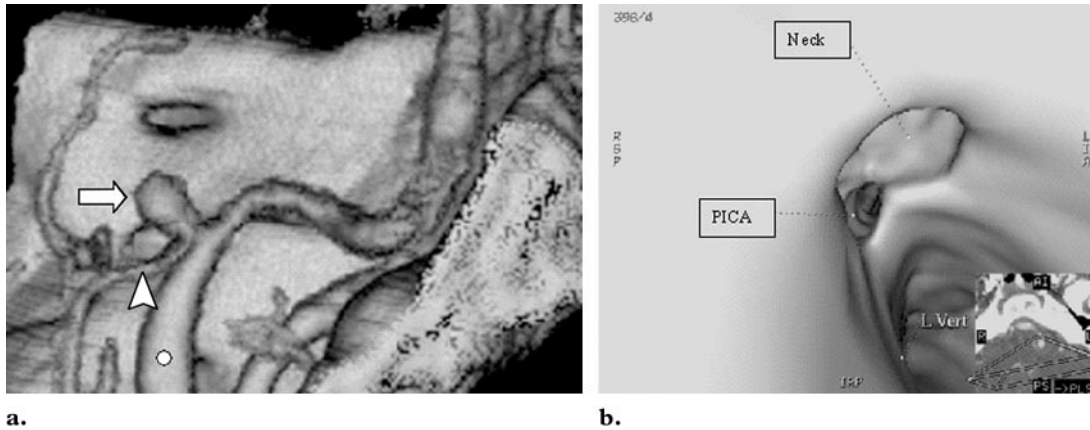


Figure 15. (a) Surface-rendered view from a multiple-row detector CT series demonstrates an aneurysm (arrow) arising at the origin of the posterior inferior cerebellar artery (arrowhead) from the vertebral artery (circle). (b) On a view from the interior of the artery, the left vertebral artery (*L Vert*), posterior inferior cerebellar artery (*PICA*), and neck of the aneurysm are all easily recognized, and their relative locations are readily appreciated. (Case courtesy of Gordon Harris, PhD, Harvard Medical School and Massachusetts General Hospital, Boston.)

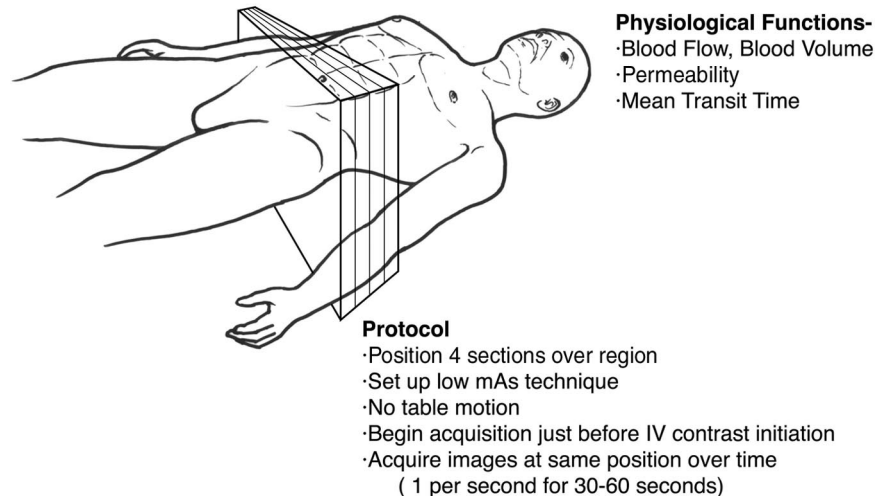


Figure 16. Diagram summarizes the CT perfusion examination. Before initiation of the CT perfusion procedure, the location of the tissue of interest must be identified. The CT sections are positioned to include this tissue, and the CT table motion is disabled. A low milliampereseconds technique is selected, and image acquisition is initiated just before intravenous injection of contrast material. A sequence of images is collected at the same table location, and these images will capture contrast material appearance and disappearance. The level of opacity in an arterial structure, as well as in the tissue of interest, is used as input to a program that computes physiologic parameters such as blood flow rate, blood volume, mean transit time, and tissue permeability.

Physiologic Imaging: CT Perfusion

CT has recently been applied to measure physiologic parameters. Tissue enhancement over time represents the rate and amount of contrast material distribution in the vascular space and extravascular, extracellular space. By using various mathematical models adjusted to the arterial at-

tenuation, measurement of tissue attenuation over time can describe physiologic parameters such as blood volume, blood flow rate, tissue permeability, and mean transit time (16). The CT acquisition series is centered over the region of interest (eg, infarct location or lesion location), and a set of images is acquired at that position (without table motion) over time as contrast material is injected, with a lower radiation dose than would be normally employed (Fig 16). (For ex-

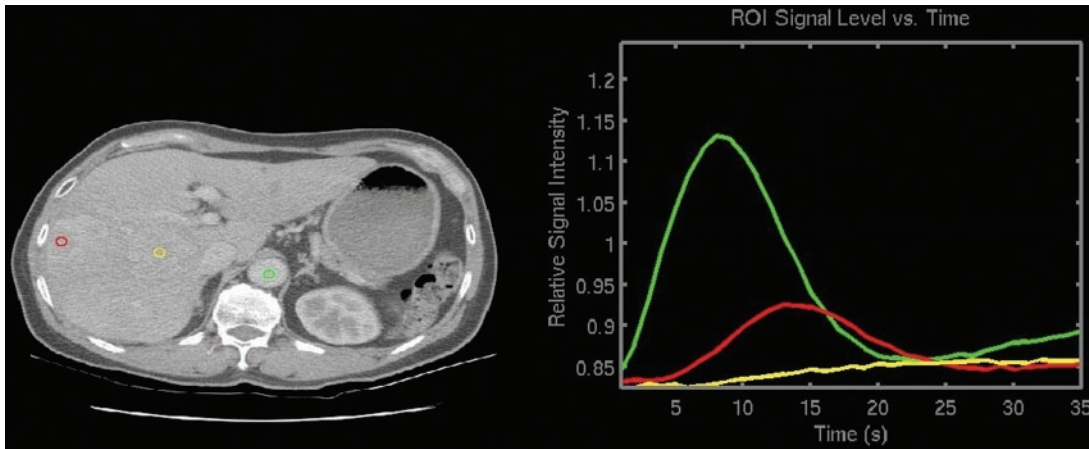


Figure 17. CT scan and time attenuation curves demonstrate an arterial flow pattern within a hepatic lesion. The aorta was used as the arterial reference vessel (green circle in the scan image and green line on the plot). The liver was sampled in two locations: unaffected normal hepatic tissue (yellow circle and yellow plot line) and hepatic tumor tissue (red circle and red plot line). The graph on the right was used to analyze the blood flow parameters for the patient by using a specific CT image-processing software package (CT Perfusion2; GE Medical Systems).

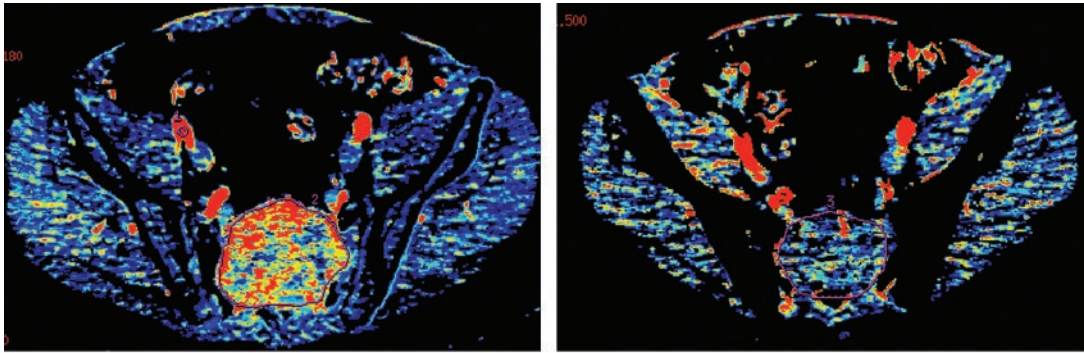


Figure 18. (a) Baseline blood flow map of a patient with an active sacral lesion shows a blood flow rate of 127.38 mL/min/100 g. (b) As shown in a blood flow map obtained 6 months after treatment, the blood flow rate has dropped to 14.15 mL/min/100 g. (Case courtesy of Chusilp Charnsangavej, MD, University of Texas M. D. Anderson Cancer Center, Houston.)

ample, a routine abdominal study for an average size patient would require 220–250 mAs at our institution. A CT perfusion study on the same patient would be obtained by using 90 mAs.) The CT numbers of several anatomic locations are sampled through the entire sequence, and the plotted results (Fig 17) form the basis for the calculation of the perfusion parameters. The parameters are generated for each voxel in the image and are typically presented as color maps. One map is generated for each section of data acquired and for each variable. These variables are considered more robust and reliable than the complementary magnetic resonance (MR) perfusion results, because CT is not burdened with as many

uniformity artifacts and image distortion problems as MR imaging. This method has been especially useful in monitoring and understanding the effect of antiangiogenic treatments for cancer (Charnsangavej C, oral communication, February 2002).

In the case shown in Figure 18, the patient had an active sacral lesion at the beginning of treatment. About 6 months later, the blood flow to the tumor region decreased to background levels. This patient and his treatment team benefited by having clear knowledge of the success of his treatment.

Conclusions

Clearly, multiple-row detector CT has initiated an explosion of new applications and very detailed data sets related to image processing. As the technology continues to develop and 8-section, 16-section, etc, CT scanners are deployed, the emergence of new applications will also continue. Turnkey image-processing workstations have become much faster and more user friendly in recent years and are providing radiologists with the tools to visualize huge data sets in vastly different ways. Future challenges include the development of simple and reliable methods for transmission and display of image-processing results to referring physicians as well as archiving these results with the original images. As soft-copy reading of digital images becomes more widespread, more radiologists will desire to do both reviewing and image-processing operations on a single workstation.

Acknowledgments: The author is extremely grateful to those individuals who contributed cases to this manuscript. Many thanks go to Gregory Gladish, MD, Eric Tamm, MD, Reginald Munden, MD, Marc Fenstermacher, MD, Chusilp Charnsangavej, MD, and Revathy Iyer, MD, from University of Texas M. D. Anderson Cancer Center. Thanks also to Gordon Harris, PhD, from Massachusetts General Hospital. Original art work was contributed by Nick M. Lang.

References

1. Baek SY, Sheafor DH, Keogan MT, DeLong DM, Nelson RC. Two-dimensional multiplanar and three-dimensional volume-rendered vascular CT in pancreatic carcinoma: interobserver agreement and comparison with standard helical techniques. *AJR Am J Roentgenol* 2001; 176:1467-1473.
2. Park SJ, Han JK, Kim TK, Choi BI. Three-dimensional spiral CT cholangiography with minimum intensity projection in patients with suspected obstructive biliary disease: comparison with percutaneous transhepatic cholangiography. *Abdom Imaging* 2001; 26:281-286.
3. Raptopoulos V, Prassopoulos P, Chuttani R, McNicholas MM, McKee JD, Kressel HY. Multiplanar CT pancreatography and distal cholangiography with minimum intensity projections. *Radiology* 1998; 207:317-324.
4. Kuszyk BS, Heath DG, Johnson PT, Eng J, Fishman EK. CT angiography with volume rendering for quantifying vascular stenoses: in vitro validation of accuracy. *AJR Am J Roentgenol* 1999; 173:449-455.
5. Wise SW, Hopper KD, Ten Have T, Schwartz T. Measuring carotid artery stenosis using CT angiography: the dilemma of artifactual lumen eccentricity. *AJR Am J Roentgenol* 1998; 170:919-923.
6. Caoili EM, Paulson EK, Heyneman LE, Branch MS, Eubanks WS, Nelson RC. Helical CT cholangiography with three-dimensional volume rendering using an oral biliary contrast agent: feasibility of a novel technique. *AJR Am J Roentgenol* 2000; 174:487-492.
7. Coll DM, Herts BR, Davros WJ, Uzzo RG, Novick AC. Preoperative use of 3D volume rendering to demonstrate renal tumors and renal anatomy. *RadioGraphics* 2000; 20:431-438.
8. Hong KC, Freeny PC. Pancreaticoduodenal arcades and dorsal pancreatic artery: comparison of CT angiography with three-dimensional volume rendering, maximum intensity projection, and shaded-surface display. *AJR Am J Roentgenol* 1999; 172:925-931.
9. Johnson PT, Halpern EJ, Kuszyk BS, et al. Renal artery stenosis: CT angiography—comparison of real-time volume-rendering and maximum intensity projection algorithms. *Radiology* 1999; 211:337-343.
10. Addis KA, Hopper KD, Iyrobos TA, et al. CT angiography: in vitro comparison of five reconstruction methods. *AJR Am J Roentgenol* 2001; 177:1171-1176.
11. Ebert DS, Heath DG, Kuszyk BS, et al. Evaluating the potential of problems of three-dimensional computed tomography measurements of arterial stenosis. *J Digital Imaging* 1998; 11:151-157.
12. Kawamoto S, Johnson PT, Fishman EK. Three-dimensional CT angiography of the thorax: clinical applications. *Semin Ultrasound CT MR* 1998; 19:425-438.
13. Johnson PT, Fishman EK, Duckwall JR, Calhoun PS, Heath DG. Interactive three-dimensional volume rendering of spiral CT data: current applications in the thorax. *RadioGraphics* 1998; 18:165-187.
14. Addis KA, Hopper KD, Iyrobos TA, Kasales CJ, Liu Y, Wise SW. Optimization of shaded surface display for CT angiography. *Acad Radiol* 2001; 8:976-981.
15. Hopper KD, Iyrobos AT, Wise SW, Neuman JD, Mauger DT, Dasales CJ. Mucosal detail at CT virtual reality: surface versus volume rendering. *Radiology* 2000; 214:517-522.
16. Mile KA, Charnsangavej C, Lee FT, Fishman EK, Horton K, Lee TY. Application of CT in the investigation of angiogenesis in oncology. *Acad Radiol* 2000; 7:840-850.